Fetch effect on the developmental process of aeolian sand transport in a wind tunnel

CHEN Zongyan[1,2], XIAO Fengjun[1*], DONG Zhibao[1]

[1] School of Geography and Tourism, Shaanxi Normal University, Xi'an 710119, China;
[2] College of Geographic Science, Qinghai Normal University, Xining 810008, China

Abstract: As the sand mass flux increases from zero at the leading edge of a saltating surface to the equilibrium mass flux at the critical fetch length, the wind flow is modified and then the relative contribution of aerodynamic and bombardment entrainment is changed. In the end the velocity, trajectory and mass flux profile will vary simultaneously. But how the transportation of different sand size groups varies with fetch distance is still unclear. Wind tunnel experiments were conducted to investigate the fetch effect on mass flux and its distribution with height of the total sand and each size group in transportation. The mass flux was measured at six fetch length locations (0.5, 1.2, 1.9, 2.6, 3.4 and 4.1 m) and at three free-stream wind velocities (8.8, 12.2 and 14.5 m/s). The results reveal that the total mass flux and the mass flux of each size group with height can be expressed by $q=a\exp(-bh)$, where q is the sand mass flux at height h, and a and b are regression coefficients. The coefficient b represents the relative decay rate. Both the relative decay rates of total mass flux and each size group are independent of fetch length after a quick decay over a short fetch. This is much shorter than that of mass flux. The equilibrium of the relative decay rate cannot be regarded as an equilibrium mass flux profile for aeolian sand transport. The mass fluxes of 176.0, 209.3 and 148.0 μm size groups increase more quickly than that of other size groups, which indicates strong size-selection of grains exists along the fetch length. The maximal size group in mass flux (176.0 μm) is smaller than the maximal size group of the bed grains (209.3 μm). The relative contribution of each size group to the total mass flux is not monotonically decreasing with grain size due to the lift-off of some small grains being reduced due to the protection by large grains. The results indicate that there are complex interactions among different size groups in the developmental process of aeolian sand transport and more attention should be focused on the fetch effect because it has different influences on the total mass flux, the mass flux profile and its relative decay rate.

Keywords: fetch length; mass flux profile; grain size distribution; sand transport; wind tunnel experiment

1 Introduction

The fetch effect is an increase of the mass flux downwind with distance from the leading edge of a saltating surface (Stout, 1990; Gillette et al., 1996; Dong et al., 2004a; Delgado-Fernandez, 2010; Lynch et al., 2016). The mass flux measured from areas where the fetch distance is shorter than the critical fetch distance will underestimate the true equilibrium mass flux. Therefore, many excellent studies exist on the effects of moisture, surface texture, gravel and other sediment-limited conditions (Gillette et al., 1996; van der Wal, 1998; Dong et al., 2004b; Bauer et al., 2009) and over

*Corresponding author: XIAO Fengjun (E-mail: xiaofengjun@snnu.edu.cn)
Received 2019-10-18; revised 2020-01-10; accepted 2020-05-10

dry loose sand bed (Shao and Raupach, 1992; Dong et al., 2004a), but most of the attention has focused on the total mass flux. However, as the mass flux increases with fetch distance and the wind flow becomes modified, the velocity and trajectory of saltating sand grains and the vertical distribution of mass flux should also vary along the fetch distance which are important parameters of some aeolian sand transport model in supply limited conditions (de Vries et al., 2014; Hoonhout and de Vries, 2016). In addition, studies have shown the mass flux profile of each size group differs largely (Arens et al., 2002; Xing, 2007; Li et al., 2008; Tan et al., 2014; Yang et al., 2019). However, the fetch effect on the transportation of different size groups in the developmental process of aeolian sand transport is scarce.

The natural sand surface is usually a mix of grains of different size groups and the transportation of each size group differs. For example, Li et al. (2008) found that the mass flux profile of 90 to 355 μm size groups can be expressed by an exponential function, while that of 355 to 1000 μm size groups follow a power function. Tan et al. (2014) found that the mass flux profile of fine sand groups (63–800 μm) can be expressed by a Gaussian peak function, while that of coarse size groups (800–2000 μm) can be described by an exponential function. Yang et al. (2019) found the mass flux of fine sand decreases slightly with height above the sand bed at wind velocities <18 m/s, but increases slightly with height at wind velocities >18 m/s, and then shows a rapid exponential decrease with height, whereas that of medium and coarse sand decrease exponentially with height. They also found the contributions of mass flux of medium and coarse sand to total mass flux increase with wind velocity. The different mass flux profiles of each size group and contributions to total mass flux will obviously have a large influence on the total mass flux profile which is the weighted superposition of mass flux profiles of all size groups and should be primarily responsible for the different total mass flux profiles, such as the exponential function (Nickling, 1983; Nalpanis et al., 1993; Rasmussen and Sørensen, 2008), the power function (Sterk and Raats, 1996) and the Gaussian peak function (Dong et al., 2004b). It also will affect the parameters of mean size, sorting, skewness and kurtosis (Arens et al., 2002; Farrell et al., 2012; Tan et al., 2014).

The developmental stage may also have some influences. At the very early stage of aeolian sand transport, aerodynamic entrainment of grains plays a major role in the dynamics of saltation and more small size grains than large size grains can be transported by wind flow. As more and more sand grains are entrained, the wind flow becomes significantly modified and the entrainment by grain bombardment quickly dominates over aerodynamic entrainment (Shao and Raupach, 1992; Bauer and Davidson-Arnott, 2003; Delgado-Fernandez, 2010). Meanwhile, sand grains absorb more momentum from the wind flow and impact the sand bed at a much larger velocity, and then they can eject more large size grains into the wind flow. Therefore, the dislodgment rate and the mass flux profile of different size groups will vary unless the true equilibrium stage is reached. Shao and Raupach (1992) found that their 14.5 m long sand bed did not meet the criteria for the stabilization of saltation. Dong et al. (2004a) also found that the total mass flux increased within their 16 m long sand bed. Therefore, the wind tunnels in most studies were probably insufficiently long to observe the whole development of aeolian sand transport, which indicated the results of many wind tunnel experiments were probably derived from some specific stage of the developmental process.

The aim of this study was to investigate the fetch effect on the developmental process of aeolian sand transport by analyzing the changes in the mass flux and its relative decay rate of total sand transport, and the relative importance and significance of each size group along the fetch distance.

2 Materials and methods

All experiments were conducted in a blow-type non-circulating wind tunnel at the School of Geography and Tourism, Shaanxi Normal University of China. The wind tunnel has a total length of 16.5 m, and the working section is 7.0 m long, 0.5 m wide and 0.6 m high. The roughness elements (78 wood blocks with dimensions of 0.02 m×0.04 m×0.04 m) were placed in front of the working section to produce a thick boundary layer. The free-stream wind velocity in the wind

tunnel can be changed continuously from 3 to 35 m/s. The thickness of the boundary layer in the working section is about 0.12 m. Figure 1 shows the layout of instrumentation for the wind tunnel experiment.

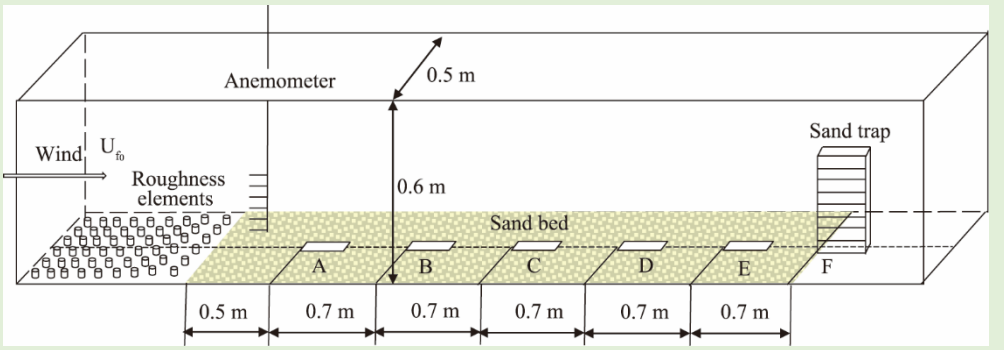

Fig. 1 Layout of the instrumentation for the wind tunnel experiment. U_{f0} is the free-stream wind velocity; and A–F are fetch length locations.

The test sand was from the Tengger Desert of China. The mean size is 0.19 mm with a standard deviation of 0.41. The critical aerodynamic entrainment wind velocity is about 6 m/s. In the experiment, a 0.029 m thick layer of sand was evenly spread on a sand tray along the wind tunnel bed. The segmented sand sampler of Dong et al. (2004c) was used to measure the sand mass flux profile. This sand trap is 0.30 m high and has 15 collection chambers (0.01 m wide and 0.02 m high). The sampler was located at six fetch length locations which were 0.5, 1.2, 1.9, 2.6, 3.4 and 4.1 m downwind from the leading edge of the sand bed at locations A–F in Figure 1. The locations are not evenly distributed because some supporting structures of the wind tunnel cannot be removed. Three free-stream wind velocities (8.8, 12.2 and 14.5 m/s) were used to measure the mass flux profiles. The sampling durations of the experiments were 1200, 420 and 300 s, which are mainly decided by the depletion of the sand bed because the sand grains at the upwind section will be blown away and the bed floor will expose after a long time experiment. Therefore, each experiment is ceased before the exposure of the bed floor to ensure the fetch distance is not changed. The durations of warm-up and cease periods are only a few seconds which are much shorter than the whole experimental duration. Therefore, their contributions to the total mass flux are negligible. For each combination of fetch length and wind velocity, three replicates were conducted to obtain mean values.

Sand samples collected by the chambers were weighed by a high-accuracy electronic scale with an accuracy of 0.001 g, and then the grain size distributions were analyzed by a Microtrac-S3500 grain size analyzer (Microtrac Inc., USA). Since the mass flux at 8.8 m/s wind velocity was very small, the relative decay rate of each size group was not calculated.

3 Results and discussion

3.1 Mass flux profile of all size groups and total mass flux

Figure 2 shows the mass flux profile of all size groups with fetch length and wind velocity. The mass flux decays exponentially in the entire vertical region for all six fetch lengths at 8.8 m/s wind velocity (Fig. 2a). At 12.2 m/s wind velocity, the mass flux tends to decay with height, but has a small negative deviation below 0.03 m (Fig. 2b). At 14.5 m/s wind velocity, the mass flux for 0.5 m fetch length is similar to that in Figure 2b. However, the mass flux for the other five fetch lengths increases with height above the sand bed, and then decays quickly with height (Fig. 2c). This is consistent with the results of some previous studies (Dong et al., 2004a; Tan et al., 2014), but differs from some other positive deviation results (Butterfield, 1999; Namikas, 2003; Li et al., 2008; Kang et al., 2016). The disagreement is partly because the intrusive sampler has difficulties in collecting all the saltating and creeping sand grains in the near bed region where the densest concentration of mass flux occurs, but this does not affect the mass flux profile above the reversal height.

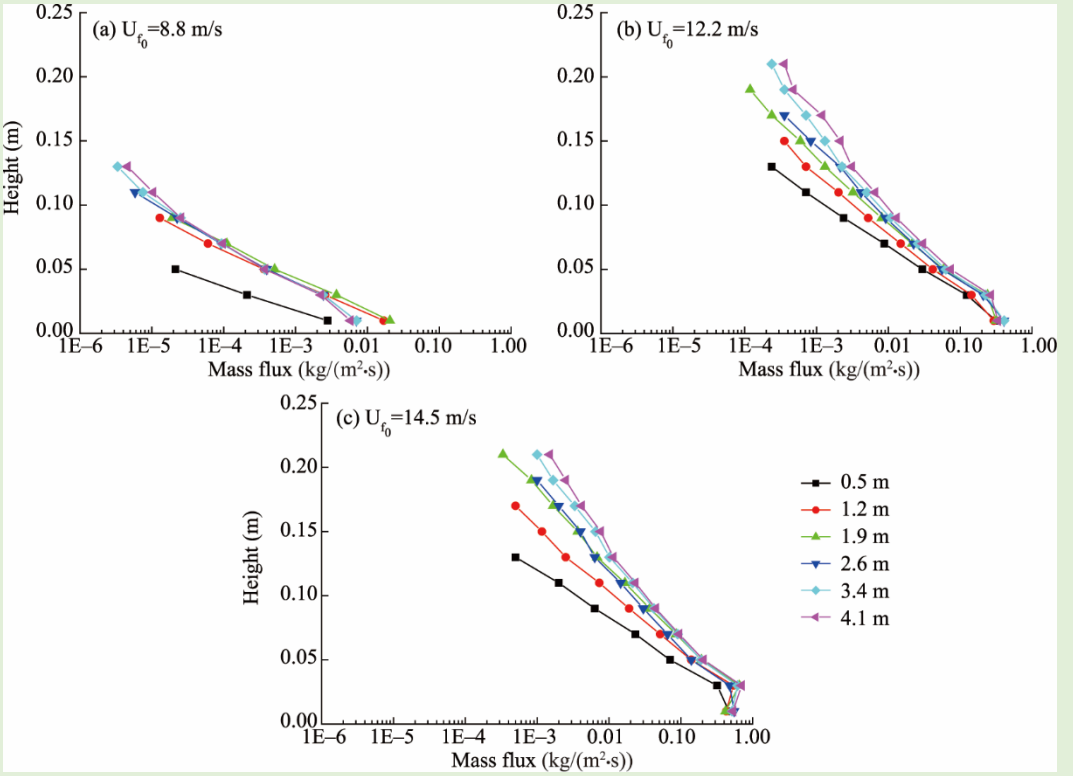

Fig. 2 Variation of the sand mass flux profiles with fetch length under different free-stream wind velocity

The vertical distribution of sand mass flux above 0.03 m can be described by the following exponential function:

$$q = a\exp(-bh), \tag{1}$$

where q is the sand mass flux (kg/(m²·s)) of all size groups at height h (m); a and b are regression coefficients. The coefficient b in Equation 1 represents the relative decay rate of the sand mass flux with height. Using the least squares curve-fit method, the relative decay rate b was calculated and is shown in Figure 3.

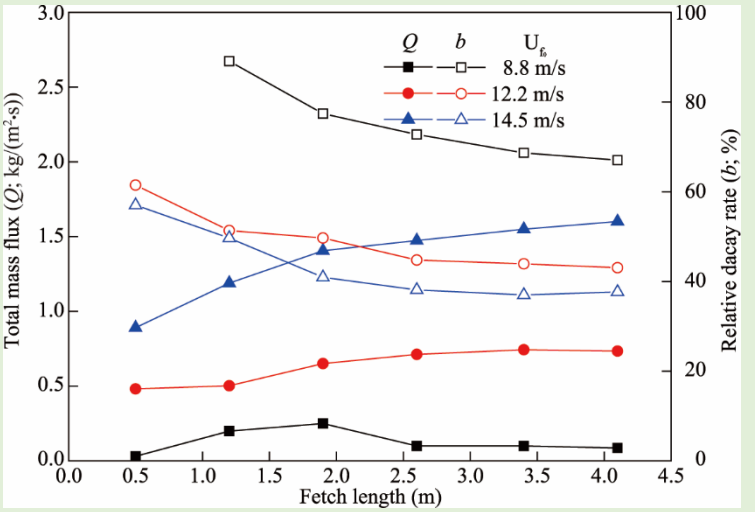

Fig. 3 Variation of the total sand mass flux and the relative decay rate with fetch length

Figure 3 shows the variation of total mass flux and the relative decay rate in Equation 1 with

fetch length. The total sand flux shows a general tendency to increase with fetch length and this tendency is increasing with the wind velocity. At 8.8 m/s wind velocity, after a quick growth and an overshooting stage, the total mass flux decreases to a constant, and seems to approach to the equilibrium stage noted by Shao and Raupach (1992). For the short working section of the wind tunnel used in this study, we cannot observe the whole tendency of total mass flux at 12.2 and 14.5 m/s wind velocities.

Both the wind velocity and fetch length affect the relative decay rate. In Figure 3, the relative decay rate b decreases with wind velocity. Apparently, this is because sand grains absorb more momentum from the stronger wind flow, have greater lift-off velocity and then can reach higher heights. Figure 3 also shows that b decreases rapidly when the fetch length is short (about 2.6 m), but then it decays much more slowly and is almost constant when the fetch reaches a certain length which is much shorter than that of the total mass flux. This is in agreement with the reported experimental results of Dong et al. (2004a) and the numerical results of Xiao et al. (2013). Dong et al. (2004a) argued that the mass flux profile reached an equilibrium stage and a stable probability distribution of lift-off velocity. However, this disagreed with their further investigations as the average saltation height increased in the whole fetch length region in their experiment. This implies the lift-off velocity still increases and sand grains can move into higher heights and the mass flux profile does not reach the true equilibrium stage.

3.2 Mass flux profile and total mass flux of each size group

The mass flux of each sand size group can be calculated by the following equation:

$$q_i = q\, f_h(d_i), \tag{2}$$

where q_i and q are the sand mass flux (kg/(m^2·s)) of grain size group d_i and the mass flux of all size groups at height h (m) (Fig. 2); d_i is the diameter (μm) of size group i; and $f_h(d_i)$ is the mass fraction of d_i at height h which was analyzed by the Microtrac-S3500 grain size analyzer.

Mass flux profiles of four size groups are shown in Figure 4. At low wind velocities and/or short fetch lengths, the mass flux decays exponentially in the whole height region, and this is consistent

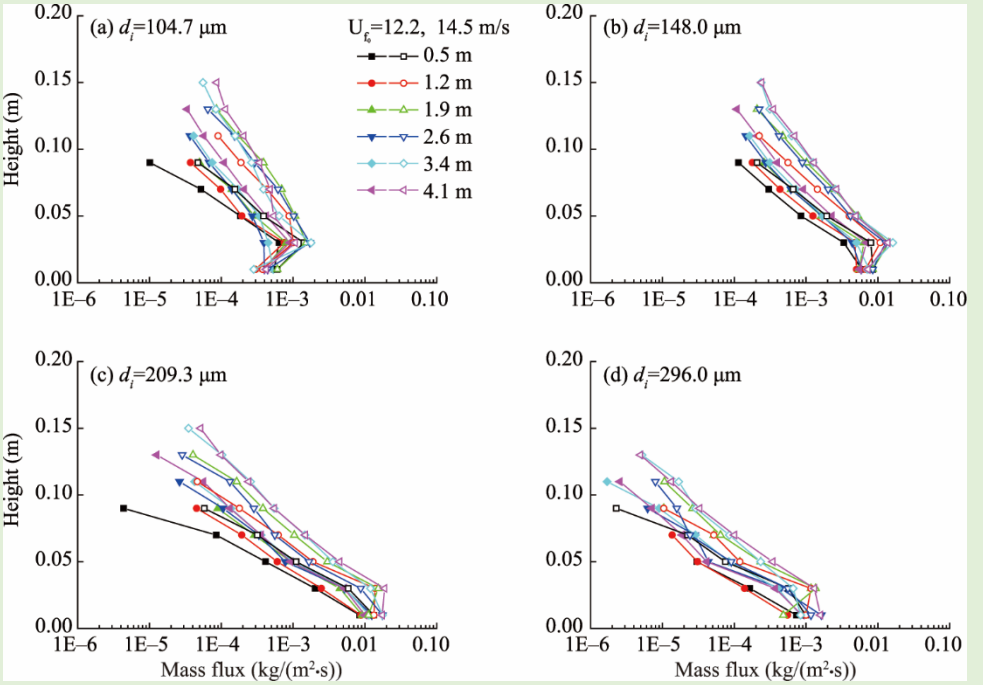

Fig. 4 Variation of the sand mass flux profiles of different grain size groups with fetch length. d_i is the diameter (μm) of a size group.

with the results from studies of loose sandy surfaces (Dong et al., 2003; Namikas, 2003) and some

gravel surfaces when the wind velocity is low (Tan et al., 2016). As the wind velocity and/or fetch length increases, the mass flux profile gradually deviates from those over a sandy surface. A peak mass flux appears at 0.03 m height, and then the mass flux decreases with height which presents the classic unimodal curve over a gravel surface (Dong et al., 2004b). However, the mass flux above 0.03 m of each size group still follows the exponential function of Equation 1.

Figure 4 also shows that the grain size greatly affects the mass flux profiles. For small sand size groups, the mass flux profile tends to show a unimodal curve, while for large sand size groups, the mass flux decreases exponentially with height. Dong et al. (2004a, b) also found that the peak mass flux height increased with both the wind velocity and the fetch length of the sand surface, but in our experiment, the peak mass flux height is a constant (0.03 m). This may be due to the larger wind velocities and fetch lengths employed in their experiment. With increasing wind velocity, the critical grain size by direct aerodynamic entrainment and the velocity of entrained sand grains increases, and then more large sand grains can be driven into the higher height.

The relative decay rate b of each size group was calculated and is shown in Figure 5. At any fetch location, b seems to decrease with increasing grain size, which indicates the mass flux of large size group decays more quickly with height than that of small size group. This agrees with the results of Li et al. (2008), though their mass fluxes of size groups (d>355 μm) follow a negative power law. The mass fraction of d>355 μm in the bed grains in our experiments is less than 5%, and the mass flux profiles of these size groups were not analyzed. b also decreases quickly at the first 1.4 m fetch length, and then tends to reach a constant value. This is similar to the relative decay rate of total mass flux in Figure 3, though it differs in grain size. The b of small size groups (e.g., 88.0 and 140.7 μm) decays more quickly than that of large size groups at this short fetch length.

Figure 5 also shows that b of total mass flux deviates significantly from b of the maximal size group of bed grains (209.3 μm) and b of the main size group in transportation (176.0 μm; Fig. 6), but it is close to some small size groups. At 12.2 m/s wind velocity, b of the total mass flux is almost equal to b of the 148.0 μm size group. At 14.5 m/s wind velocity, b of the total mass flux is also close to the b of 148.0 μm size group when fetch length is less than 2.6 m, but then it is approaching to the 176.0 μm size group. At the same time, the variation amplitude of b is changed with grain size as it may be seen that the curves of 124.5, 148.0, 176.0 and 209.3 μm are more smoothly than others. This is attributable to the different mass fraction contributions of each size group to the total mass flux. The larger deviations of measured q_i of the size groups less transported in the wind flow will lead to the relatively greater fluctuations in b.

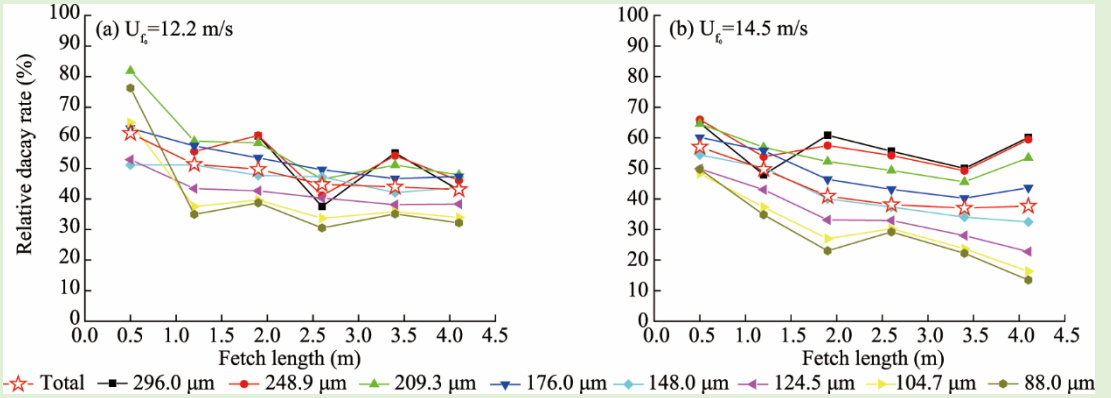

Fig. 5 Variation of the relative decay rate of different size groups with different fetch length locations. Total means the relative decay rate of total sand.

Figure 6 shows the total mass flux of different size groups Q_i with fetch length, where Q_i is calculated by integrating the mass flux with height according to the mass flux profile of different size groups. Firstly, we find that Q_i of the 176.0, 209.3 and 148.0 μm size groups are the main components of the total mass flux Q, but Q_i of the 176.0 μm size group is greater than Q_i of the 209.3 μm size group (maximal size group in the bed grains). Secondly, the increasing rates of these

three size groups with fetch length are greater than those of other size groups whose contributions are small but cannot be neglected. The total mass flux Q is the weighted superposition of Q_i of all grain size groups, and it is same to the total mass flux profile. The different increasing rate of each size group with fetch also shows the ratio of mass flux of each size group at different fetch lengths varies significantly. It is inconsistent with the results of Yang et al. (2019), who found the weight percentage of each size group in transportation is in accordance with the weight percentage in the bed grains. This is because the four size groups (very fine, fine, medium and coarse) in their study will probably mask some detailed information as there are eight size groups in this study.

These results are contrary to the independent assumption of Shao et al. (1996), who assumed that the transportation of different size groups behaves independently and the mass flux of each size group is unaffected by other groups. These results also indicate that the median or mean grain size of bed grains is not suitable to represent all grain size groups in transportation.

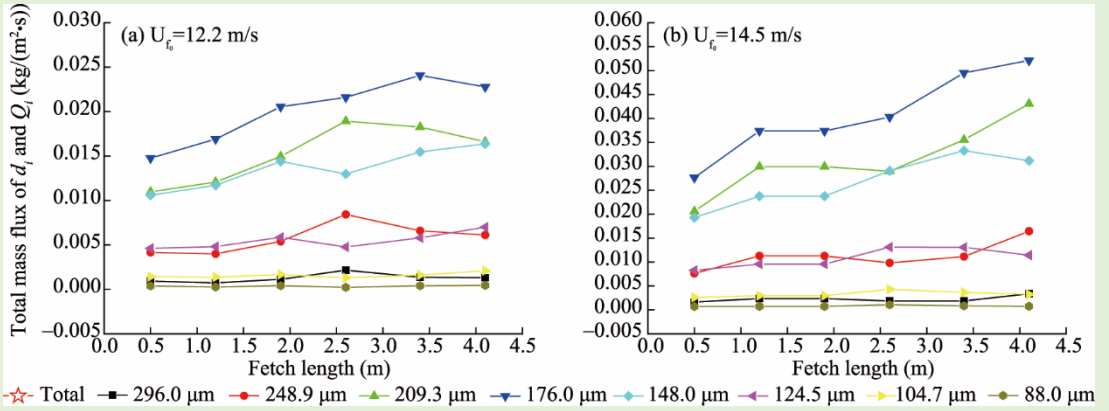

Fig. 6 Variation of the total mass flux (Q_i) of different size groups (d_i) with different fetch length

3.3 Mean grain size profile

The mean grain size profile is an important parameter to validate aeolian sand transport models and is a reflection of the grain trajectory and lift-off velocity. Figure 7 shows that mean grain size d_m decreases with the height in each experiment and has a weak increasing trend with fetch, which agrees with the widely accepted conclusion by many studies. Jensen and Sørensen (1986) and Rice et al. (1995) found that large grains launched at lower speeds and angles than small grains from wind tunnel experiments. Xiao et al. (2012) also found that the mean horizontal velocity of a small size group is larger than that of large size group at any height in their numerical simulation. Apparently, the mean lift-off velocity of saltating sand grains decreases with grain size, and therefore its probability of reaching a higher height reduces as evidenced by the grain-size distributions in Figure 8. But this disagrees with the results of Tan et al. (2014) and Yang et al. (2019), who found that d_m decreases with height at first and then shows an increase with the height, and the height of the reversal point increases with wind velocity. This difference may be because of the different measurement heights of mass flux and the different grain size distributions of bed grains in each experiment. The maximum height in the study of Tan et al. (2014) was 0.60 m and that of Yang et al. (2019) was 0.50 m, whereas it is between 0.05 and 0.25 m in this study according to the fetch length and wind velocity. The test sand of Tan et al. (2014) and Yang et al. (2019) contained more medium sand (250–500 μm) and coarse sand (500–1000 μm), which makes the sand transport similar to that on a gravel sand surface.

Figure 8 shows the trend of $f_{h,i}/f_{bed,i}$ at different heights at 14.5 m/s wind velocity and 4.1 m fetch length. Here $f_{h,i}/f_{bed,i}$ is the ratio of the mass fraction of a certain size group d_i in transportation ($f_{h,i}$) to that in the bed grains ($f_{bed,i}$). The greater the value of $f_{h,i}/f_{bed,i}$, the more the relative contribution to the mass flux. It may be observed that the relative contribution of small size groups increases with height (Fig. 8), which shows that mean grain size decreases with height as shown in Figure 7.

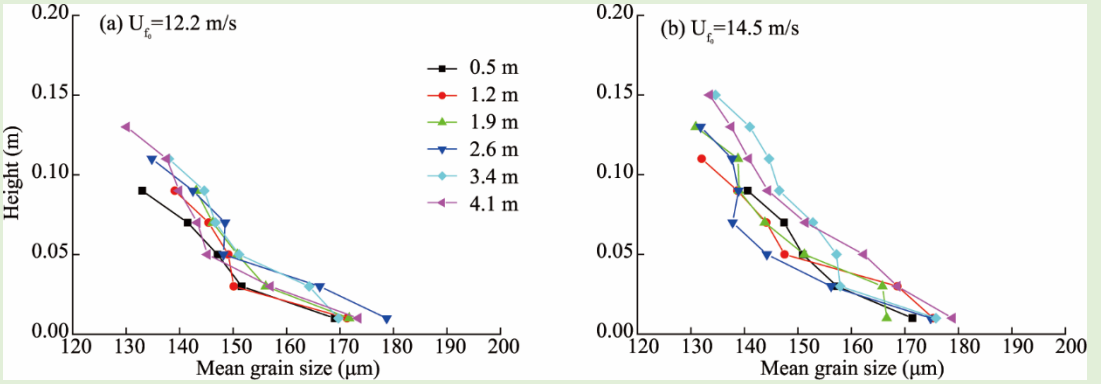

Fig. 7 Variation of the mean grain size with fetch length

Figure 8 also shows that $f_{h,i}/f_{bed,i}$ is not monotonically decreasing with grain size. At 0.01 m height, the values of $f_{h,i}/f_{bed,i}$ of the 124.5,148.0,176.0 and 209.3 μm size groups are larger than 1 (the red line; Fig. 8), whereas it is less than 1 for other size groups, especially the 88.0 and 104.7 μm size groups. At 0.03–0.09 m, the maximum value of $f_{h,i}/f_{bed,i}$ is at the 104.7 μm size group, and then drops to the 88.0 μm size group at 0.11 and 0.13 m heights. It is more likely due to the shielding effect of large grains and the reduced wind speed near the bed rather than the cohesive forces. The cohesive forces are only important to grains less than 70 μm, which make the threshold wind velocity higher (Greeley and Iversen, 1985). Large grains can protect the underlying grains from bombardment by impacting sand grains and direct entrainment by wind flow which is partly similar to the effect of gravels on sand transport (Dong et al., 2004b; Gillies et al., 2007).

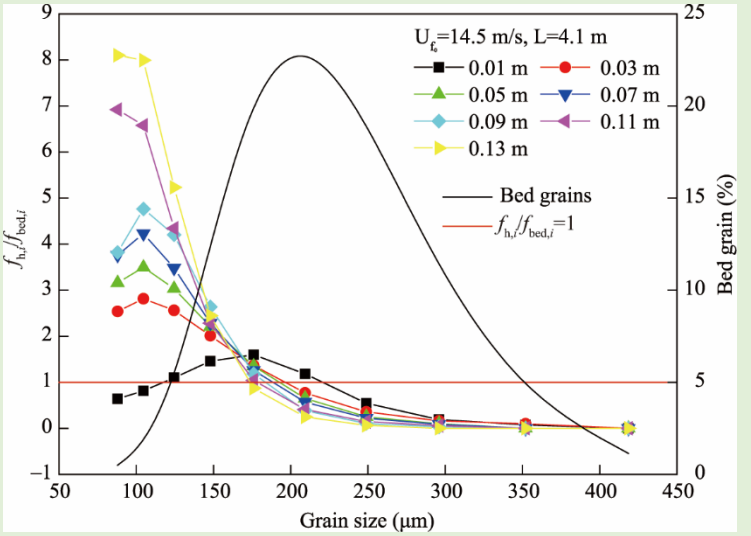

Fig. 8 Trend of $f_{h,i}/f_{bed,i}$ at different heights and with grain-size distribution of bed grains. $f_{h,i}/f_{bed,i}$ is the ratio of the mass fraction of a certain size group (d_i) in transportation ($f_{h,i}$) to that in the bed grains ($f_{bed,i}$). L, fetch length.

Wind velocity has a similar effect on the interactions among each size group as that of fetch length. The critical grain size by direct aerodynamic entrainment and the velocity of entrained sand grains increases with the increase in wind velocity, and then more large sand grains can be driven into the wind flow. The strong size-selection of grains indicates that there are complex interactions among different size groups at least in the developmental process of aeolian sand transport though the relative decay rates of total mass flux and each size group have reached a constant.

The wind tunnel dimension constraint will affect aeolian sand transport. The dimensions of the wind tunnel are important factors in determining whether or not the accurate modeling of saltation has been made. If choked saltation occurs, the wind tunnel constraint will alter the wind flow and

the mass flux profile. Owen and Gillette (1985) investigated the wind tunnel size constraint on the development of saltation and suggested that the Froude number should be less than 20. The Froude number was defined as $Fr=U^2/(g\mathrm{H})$, where U is free-stream wind speed, g is the gravitational acceleration, and H is the height of the wind tunnel. White and Mounla (1991) suggested a more conservative Froude number value of 10 to ensure the accurate saltation tunnel simulation by analyzing the variations of friction velocity as a function of the downstream position in a wind tunnel and using walnut shells as test grains. The light density of walnut shells would greatly cut down the critical entrainment wind velocity and the critical Froude number. However, it seems difficult and even impossible to meet the Froude number criteria. According to the suggested values of Owen and Gillette (1985), and White and Mounla (1991), the free-stream velocity of our wind tunnel should be less than 10.8 and 7.7 m/s, respectively. This is only slightly greater than the critical aerodynamic entrainment wind velocity of test sands in this study. In addition, the critical aerodynamic entrainment wind velocities for some coarser sands will be larger than the suggested critical wind velocity. Therefore, further study is needed to investigate the wind tunnel constraint effect, but it is beyond the scope of this paper.

The results in this study have shown that the fetch effect has different influences on total mass flux and mass flux profile of each size group along the fetch distance. In addition, the dimension constraint effect of each wind tunnel is very likely to be different. Therefore, attention should be paid in wind tunnel experiments. If someone focuses on the decay rate of the mass flux profile, a short fetch distance will meet the need. But if someone focuses on the transportation of the developmental or equilibrium stage, the working section must be longer than the critical fetch length of the wind tunnel.

4 Conclusions

Changes in mass flux and the relative decay rate of total sand flux, and changes in each size group in the aeolian transport developmental process were examined in a wind tunnel. The main findings are as follows:

(1) The relative decay rates of total sand flux and in each size group decrease quickly with fetch length when the fetch is short, and then they reach the equilibrium stage. The equilibrium fetch length of the relative decay rate is much shorter than that of mass flux, indicating the equilibrium of relative decay rate cannot be regarded as the representation of the equilibrium mass flux profile and aeolian sand transport. The mass flux of the large size group decreases more quickly than that of small size groups in all experiments.

(2) The mass flux of each size group increases asynchronously with fetch length. The mass fluxes of the 176.0, 209.3 and 148.0 μm size groups increase more quickly than that of other size groups.

(3) Mean grain size decreases with height and slightly increases with fetch length.

(4) The maximal size group in transportation (176.0 μm) is smaller than the maximal size group in the bed grains (209.3 μm). The relative contribution to total mass flux does not increase with decreasing sand size. The protection effect of large grains on small grains will reduce their possibility of lift off from sand bed.

Our findings may deepen the understanding of interactions among different grain size groups and fetch effect on aeolian sand transport. However, the short working section of our wind tunnel makes both the total mass flux and sand mass flux profile do not reach their equilibrium stages which limit the inferences of our findings to the wholly developmental process of aeolian sand transport. Attention should be paid in wind tunnel experiments because of the different influences of fetch effect on the total mass flux, the mass flux profile and its relative decay rate.

Acknowledgements

This research was supported by the National Natural Science Foundation of China (41601002, 41871011), the China Postdoctoral Science Foundation (2017M623115), the Science Foundation of Shaanxi Province (2018JQ4010) and the Fundamental Research Funds for the Central Universities (GK201903077). The paper was

written while the corresponding author held a visiting position in the BEADS Lab at Flinders University, Australia. Thanks to Professor Patrick HESP and the BEADS Lab for support.

References

Arens S M, van Boxel J H, Abuodha J O Z. 2002. Changes in grain size of sand in transport over a foredune. Earth Surface Processes and Landforms, 27(11): 1163–1175.

Bauer B O, Davidson-Arnott R G D. 2003. A general framework for modeling sediment supply to coastal dunes including wind angle, beach geometry, and fetch effects. Geomorphology, 49(1–2): 89–108.

Bauer B O, Davidson-Arnott R G D, Hesp P A, et al. 2009. Aeolian sediment transport on a beach: Surface moisture, wind fetch, and mean transport. Geomorphology, 105(1–2): 106–116.

Butterfield G R. 1999. Near-bed mass flux profiles in aeolian sand transport: High-resolution measurements in a wind tunnel. Earth Surface Processes and Landforms, 24(5): 393–412.

de Vries S, Arens S M, de Schipper M A, et al. 2014. Aeolian sediment transport on a beach with a varying sediment supply. Aeolian Research, 15: 235–244.

Delgado-Fernandez I. 2010. A review of the application of the fetch effect to modelling sand supply to coastal foredunes. Aeolian Research, 2(2–3): 61–70.

Dong Z B, Liu X P, Wang H T, et al. 2003. The flux profile of a blowing sand cloud: a wind tunnel investigation. Geomorphology, 49(3–4): 219–230.

Dong Z B, Wang H T, Liu X P, et al. 2004a. The blown sand flux over a sandy surface: a wind tunnel investigation on the fetch effect. Geomorphology, 57(1–2): 117–127.

Dong Z B, Wang H T, Liu X P, et al. 2004b. A wind tunnel investigation of the influences of fetch length on the flux profile of a sand cloud blowing over a gravel surface. Earth Surface Processes and Landforms, 29(13): 1613–1626.

Dong Z B, Sun H Y, Zhao A G. 2004c. WITSEG sampler: a segmented sand sampler for wind tunnel test. Geomorphology, 59(1–4): 119–129.

Farrell E J, Sherman D J, Ellis J T, et al. 2012. Vertical distribution of grain size for wind blown sand. Aeolian Research, 7: 51–61.

Gillette D A, Herbert G, Stockton P H, et al. 1996. Causes of the fetch effect in wind erosion. Earth Surface Processes and Landforms, 21(7): 641–659.

Gillies J A, Nickling W G, King J. 2007. Shear stress partitioning in large patches of roughness in the atmospheric inertial sublayer. Boundary-Layer Meteorology, 122(2): 367–396.

Greeley R, Iversen J D. 1985. Wind as a Geological Process on Earth, Mars, Venus and Titan. New York: Cambridge University Press, 333.

Hoonhout B M, de Vries S. 2016. A process-based model for aeolian sediment transport and spatiotemporal varying sediment availability. Journal of Geophysical Research: Earth Surface, 121(8): 1555–1575.

Jensen J I, Sørensen M. 1986. Estimation of some aeolian saltation transport parameters: a re-analysis of Williams' data. Sedimentology, 33(4): 547–558.

Kang L Q, Zou X Y, Zhao G D, et al. 2016. Wind tunnel investigation of horizontal and vertical sand fluxes of ascending and descending sand particles in aeolian sand transport. Earth Surface Processes and Landforms, 41(12): 1647–1657.

Li Z S, Feng D J, Wu S L, et al. 2008. Grain size and transport characteristics of non-uniform sand in aeolian saltation. Geomorphology, 100(3–4): 484–493.

Lynch K, Jackson D W T, Cooper J A G. 2016. The fetch effect on aeolian sediment transport on a sandy beach: a case study from Magilligan Strand, Northern Ireland. Earth Surface Processes and Landforms, 41(8): 1129–1135.

Nalpanis P, Hunt J C R, Barrett C F. 1993. Saltating particles over flat beds. Journal of Fluid Mechanics, 251: 661–685.

Namikas S L. 2003. Field measurement and numerical modelling of aeolian mass flux distributions on a sandy beach. Sedimentology, 50(2): 303–326.

Nickling W G. 1983. Grain-size characteristics of sediment transported during dust storms. Journal of Sedimentary Petrology, 55(5): 1011–1024.

Owen P R, Gillette D A, 1985. Wind tunnel constraint on saltation. In: Proceedings of the International Workshop on the Physics of Blown Sand. Aarhus: University of Aarhus, 253–269.

Rasmussen K R, Sørensen M. 2008. Vertical variation of particle speed and flux density in aeolian saltation: Measurement and modeling. Journal of Geophysical Research-Earth Surface, 113(F2): S12.

Rice M A, Willetts B B, McEwan I K. 1995. An experimental-study of multiple grain-size ejecta produced by collisions of

saltating grains with a flat bed. Sedimentology, 42(4): 695–706.

Shao Y P, Raupach M R. 1992. The overshoot and equilibration of saltation. Journal of Geophysical Research: Atmospheres, 97(D18): 20559–20564.

Shao Y P, Raupach M R, Leys J F. 1996. A model for predicting aeolian sand drift and dust entrainment on scales from paddock to region. Australian Journal of Soil Research, 34(3): 309–342.

Sterk G, Raats P A C. 1996. Comparison of models describing the vertical distribution of wind-eroded sediment. Soil Science Society of America Journal, 60(6): 1914–1919.

Stout J E. 1990. Wind erosion within a simple field. Transactions of the ASAE, 33(5): 1597–1600.

Tan L H, Zhang W M, Qu J J, et al. 2014. Variation with height of aeolian mass flux density and grain size distribution over natural surface covered with coarse grains: A mobile wind tunnel study. Aeolian Research, 15: 345–352.

Tan L H, Zhang W M, Qu J J, et al. 2016. Aeolian sediment transport over gobi: Field studies atop the Mogao Grottoes, China. Aeolian Research, 21: 53–60.

van der Wal D. 1998. Effects of fetch and surface texture on aeolian sand transport on two nourished beaches. Journal of Arid Environments, 39(3): 533–547.

White B, Mounla H, 1991. An experimental study of Froude number effect on wind-tunnel saltation. Aeolian Grain Transport, 1: 145–157.

Xiao F J, Guo L J, Li D B, et al. 2012. Discrete particle simulation of mixed sand transport. Particuology, 10(2): 221–228.

Xiao F J, Guo L J, Li D B, et al. 2013. Modeling the evolution of aeolian sand transport in a wind tunnel. AIP Conference Proceedings, 1547(758). doi: 10.1063/1.4816930.

Xing M. 2007. The harmonious character in equilibrium aeolian transport on mixed sand bed. Geomorphology, 86(3–4): 230–242.

Yang Y Y, Liu L Y, Li X Y, et al. 2019. Aerodynamic grain-size distribution of blown sand. Sedimentology, 66(2): 590–603.